

# Fission barriers of doubly charged silver clusters

S. Krückeberg<sup>1,a,b</sup>, G. Dietrich<sup>2,c</sup>, K. Lützenkirchen<sup>2,d</sup>, L. Schweikhard<sup>1</sup>, C. Walther<sup>2,e</sup>, and J. Ziegler<sup>1,f</sup>

<sup>1</sup>Institut für Physik, Johannes Gutenberg-Universität, D-55099 Mainz, Germany

<sup>2</sup>Institut für Kernchemie, Johannes Gutenberg-Universität, D-55099 Mainz, Germany

Received: 31 August 1998 / Received in final form: 14 January 1999

**Abstract.** The monomer evaporation energies and fission barriers of doubly charged silver cluster ions in the size range  $9 \leq n \leq 25$  are measured by collision induced dissociation. They are compared to the dissociation energies of singly charged silver clusters. A macroscopic liquid drop model combined with empirical microscopic corrections successfully describes the measured fission barriers.

**PACS.** 36.40.Qv Stability and fragmentation of clusters – 36.40.Wa Charged clusters

## 1 Introduction

Multiply charged clusters have been observed for several decades and many species have been reported during the years [1]. Recently, much experimental and theoretical work has been concentrated on metal clusters [2]. One of the central questions is the stability of small multiply charged clusters against coulombic explosion.

Several measurements have been performed concerning the fragmentation pathways of doubly charged metal clusters. It has been observed that large systems evaporate neutral atoms while smaller clusters undergo fission, i.e. decay into two charged fragments. In general, this charge-symmetric fission is highly mass-asymmetric and of the form  $M_n^{2+} \rightarrow M_{n-3}^+ + M_3^+$ . This behaviour has been first found for alkali-metal clusters [3] and gold clusters [4]. The latter results were confirmed by Penning trap experiments [5, 6] and the investigations have been extended to doubly charged silver clusters [7]. The dominant fragmentation pathways are neutral monomer evaporation for  $n > 16$  and trimer fission for most clusters with  $n \leq 16$ . However,  $Ag_{11}^{2+}$  and  $Ag_{15}^{2+}$  undergo monomer evaporation. Previous sputter experiments [8] could be reinterpreted in terms of sequential decays [7].

However, little is known so far about the dissociation energies of multiply charged metal clusters, i.e. in the case of neutral monomer evaporation the energy required for the separation of a neutral atom and in the case of fission the energy required for the decay into two charged particles (the fission barrier). The only exceptions come from a kinetic energy release study of  $Li_{26}^{2+}$  by C. Bréchnignac *et al.* [9] and investigations of doubly and triply charged gold clusters [10]. In the following we present the dissociation energies of doubly charged silver clusters as determined by collision induced dissociation (CID) in a Penning trap.

## 2 Experimental setup and procedure

Detailed descriptions of the Penning trap system have been published recently [11–13]. The experimental procedure is demonstrated in Fig. 1 for the case of CID of  $Ag_{23}^{2+}$  by time-of-flight (TOF) spectra of the cluster ensemble in the trap at different stages of the experiment. Metal cluster ions are produced by a laser vaporization source and transferred into a hyperbolic Penning trap. Mass selective quadrupole cooling is applied to accumulate and center the externally created clusters in the trap (Fig. 1a). The clusters are subsequently bombarded for 600 ms with 150-eV electrons. Thus the clusters may be transferred to higher charge states [5, 14], in the present case  $z = 2$  (Fig. 1b). Next, an ion ensemble of a specific cluster size-over-charge ratio,  $n/z$ , is selected by radial ejection of all other ions (Fig. 1c). For CID the cyclotron motion of the cluster ions is excited by a 1-ms resonant excitation and an argon gas pulse is directed into the trap volume. A storage period of 270 ms allows the clusters to collide with the argon atoms and to decay to smaller cluster sizes. The charged reaction products remain stored in the trap until the surviving precursors and the fragment ions are axially ejected and analyzed by TOF mass spectrometry. Single ion detec-

<sup>a</sup> Part of the doctoral thesis of S. Krückeberg

<sup>b</sup> *Present address:* The Rowland Institute for Science, 100 E.H. Land Blvd., Cambridge, MA 02142, USA, e-mail: [krueckeberg@rowland.org](mailto:krueckeberg@rowland.org)

<sup>c</sup> *Present address:* Landesbank Rheinland-Pfalz, Große Bleiche 54–56, D-55098 Mainz, Germany

<sup>d</sup> *Present address:* Institut de Recherches Subatomiques, Chimie Nucleaire, B.P. 28, F-67037 Strasbourg, France

<sup>e</sup> *Present address:* INE, Forschungszentrum Karlsruhe GmbH, Postfach 3640, D-76021 Karlsruhe, Germany

<sup>f</sup> *Present address:* Deutsche Bank AG, Alfred-Herrhausen-Allee 16-24, D-65760 Eschborn, Germany

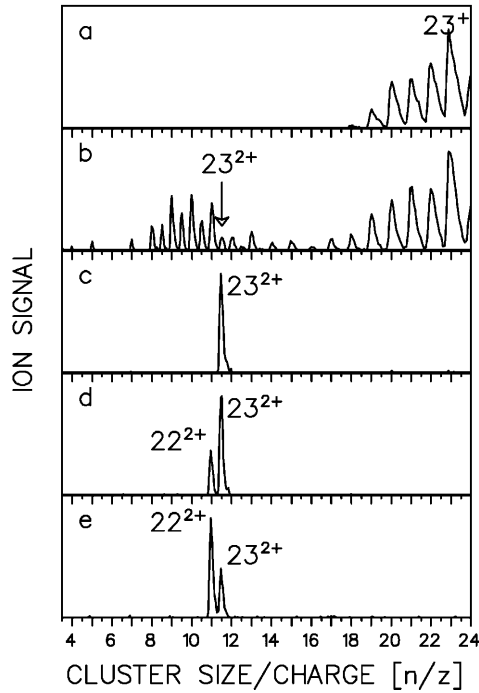


**Fig. 1.** TOF spectra showing the cluster ensemble in the trap at different stages of the experimental sequence for CID of  $\text{Ag}_{23}^{2+}$ . All  $y$  axes have been scaled to the highest signal. For details see text.

tion is performed by use of a conversion dynode detector. During the electron bombardment the residual gases, including pumping liquids from diffusion pumps, are ionized and result in large background intensities in the mass range up to  $400u$ . Therefore, only the fragmentation pattern for  $n/z \geq 4$  is analyzed.

Examples of the CID spectra of  $\text{Ag}_{23}^{2+}$  are given in Fig. 1d ( $E_{\text{kin}} = 25$  eV) and Fig. 1e ( $E_{\text{kin}} = 32$  eV). The fragmentation pathway is identified as neutral monomer evaporation:  $\text{Ag}_{23}^{2+} \rightarrow \text{Ag}_{22}^{2+} + \text{Ag}$ . The background mentioned as well as the production rates have limited the lowest size for  $\text{Ag}_n^{2+}$  to  $n = 9$ . Clusters up to size  $n = 25$  have been investigated.

For the determination of dissociation energies the fragment yield is measured as a function of the initial kinetic energy of the cluster ensemble (Fig. 2). The data analysis includes two main steps: (1) An evaluation as to which fraction of the kinetic energy  $E_{\text{kin}}$  is converted in the collisional process to excitation energy  $E_{\text{exc}}$  of the clusters. (2) A statistical model to describe the relation between this excitation energy, the dissociation energy and the fragment yield at a time  $T_{\text{D}}$  after excitation. A detailed description of these procedures is presented elsewhere [15].

In short, for the first step, a linearized version of the Impulsive Collision Theory [16] is used. Taking  $m$  as the mass of the monomer,  $m_{\text{g}}$  as the mass of the gas atoms and  $T = 300$  K as the initial internal cluster temperature, it yields:

$$E_{\text{exc}} = C^{\text{Mat}} \cdot \frac{m_{\text{g}}}{m_{\text{g}} + m} \cdot E_{\text{kin}} + (3n - 6) \cdot k_{\text{B}} \cdot T. \quad (1)$$

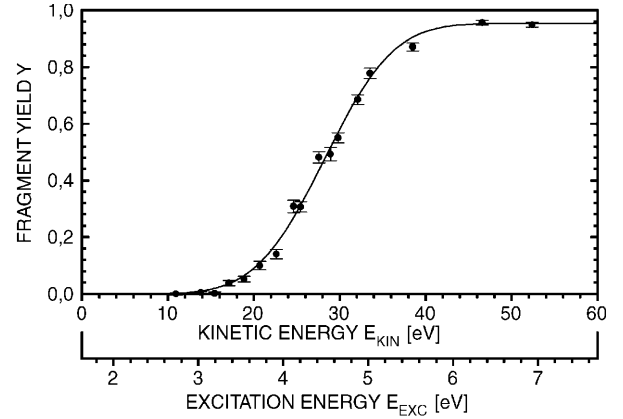


**Fig. 2.** Fragment yield of  $\text{Ag}_{23}^{2+}$  as a function of the initial kinetic energy of the clusters (upper  $x$  scale) and as a function of the resulting excitation energy (lower  $x$  scale). For details see text.

A material dependant factor  $C^{\text{Mat}}$  has to be introduced as already demonstrated for the case of silicon clusters [17]. By comparing CID results with other methods, e.g. time-resolved photofragmentation in the Penning trap [18], one obtains for silver  $C^{\text{Mat}} = 0.375$  (and thus the lower  $x$  scale of Fig. 2).

For the second step, the quantum version of the RRK model [19] is used. With the vibrational frequency  $\nu_0$  ( $\nu_0 = 4.5 \times 10^{12}$  Hz for the case of silver) the quantized excitation energy is given by  $E_{\text{exc}} = p h \nu_0$  and the dissociation energy is given by  $E_0 = q h \nu_0$ . Thus the fragment yield can be described as:

$$Y(E_{\text{exc}}) = 1 - e^{-T_{\text{D}} k(E_{\text{exc}})}. \quad (2)$$

$$k(E_{\text{exc}}) = n \cdot \nu_0 \cdot \frac{p!(p - q + 3n - 7)!}{(p + 3n - 7)!(p - q)!}. \quad (3)$$

The combination of these procedures leads to a fit of a theoretical curve to the experimental data and yields the dissociation energy as one of the fit parameters, e.g. in the case of  $\text{Ag}_{23}^{2+}$  the result is  $E_0 = (2.0 \pm 0.1)$  eV.

### 3 Experimental results

Before discussing the dissociation energies of doubly charged silver clusters, it is useful to review some of the results obtained for **singly** charged silver clusters, as displayed in Fig. 3 (top). (For a detailed analysis see [15].) The dissociation energies show two main features: (1) An odd-even staggering with odd-size clusters having a higher stability than even-size clusters. (2) The cluster sizes  $n = 9$  and 21 have an outstandingly high dissociation energy, especially in comparison to the next larger neighbour. All clusters decay by evaporation of a neutral atom, except for  $\text{Ag}_{11}^{+}$  which emits a dimer [20].

The fragmentation pathways of **doubly** charged silver clusters have already been mentioned in the introduction; they are described in detail elsewhere [7]. For the dissociation energies depicted in Fig. 3 (middle) several features

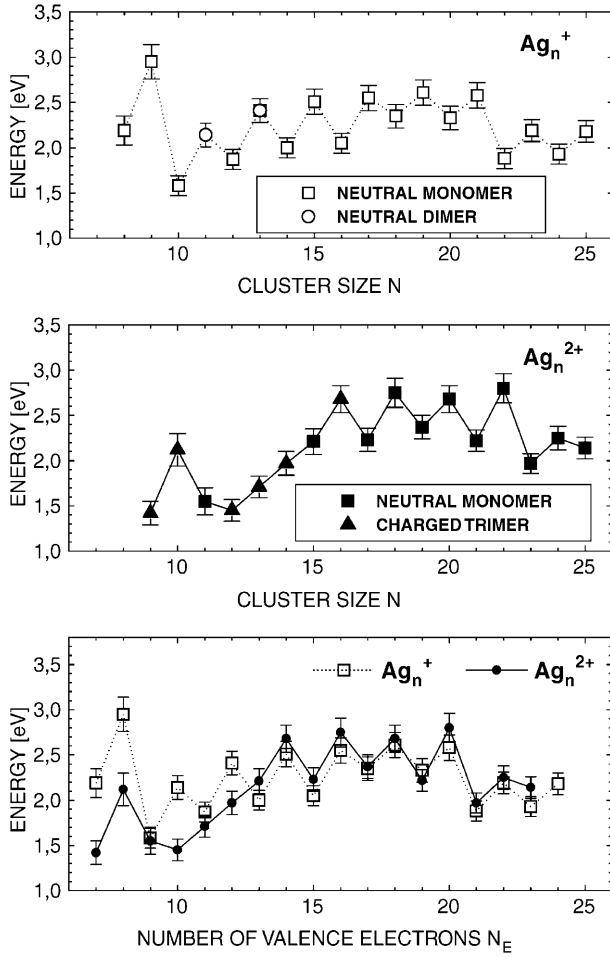


**Fig. 3.** Dissociation energies of  $\text{Ag}_n^{z+}$ . Top: singly charged clusters ( $z = 1$ ). Middle: doubly charged clusters ( $z = 2$ ). Bottom: Comparison of the dissociation energies as a function of the number of valence electrons  $n_e = n - z$ .

can be observed: (1) For clusters with  $n \geq 16$  an odd-even-staggering is observed, but now the even-size clusters are more stable than their odd-size neighbours. (2) Below  $n = 16$  this staggering vanishes for the fissioning clusters  $n = 12 - 16$ . (3) Cluster sizes of outstanding stability are  $\text{Ag}_{10}^{2+}$  and  $\text{Ag}_{22}^{2+}$ .

From these observations, the main features seem to be a function of the number of valence electrons  $n_e = n - z$ . Therefore, the dissociation energies are plotted as a function of  $n_e$  in Fig. 3 (bottom). Cluster sizes with an even number of valence electrons have a higher stability than their odd- $n_e$  neighbours and special stabilities occur at  $n_e = 8$  and  $20$ .

#### 4 Discussion in terms of a macroscopic-microscopic model

The liquid drop model [21] in which the total energy of the cluster is given in terms of a volume-, surface-,

and Coulomb-energy provides a macroscopic approach to the properties of metal clusters. The constants of the parametrization are taken from bulk material properties [2, 22]. The dissociation energy for the emission of a neutral particle is given as the difference between the total energy of the initial and the total energies of the final states. For the dissociation energy in the case of fission (fission barrier) the Coulomb wall has to be taken into account which is calculated in a touching sphere model [2].

The expected dissociation energies for monomer evaporation and trimer fission are presented in Fig. 4 (top). For clusters below  $n = 14$  the fission is energetically preferred. This goes along with the observed fission for most small silver clusters. However, the exceptional monomer evaporation of  $\text{Ag}_{11}^{2+}$  and the details of the measured dissociation energies are not explained.

Only more advanced calculations can account for the electronic and geometric structure of the clusters, i.e. the microscopic effects. The stabilities at  $n_e = 8$  and  $20$  can be understood qualitatively as shell closures in a spherical jellium model [21] and the odd-even staggering can be explained in terms of the Jahn-Teller effect [23]. However, quantitative theoretical calculations of structures and binding energies of silver clusters have been published only for the size range  $n \leq 9$  and charge states  $z = -1, 0$  and  $1$  [24].

Therefore, we present a different approach: The difference between the **measured** dissociation energy of a **singly** charged silver cluster  $\text{Ag}_n^+$  and the prediction of the liquid drop model for the decay of this cluster is used to deduce empirical microscopic corrections ( $E_{\text{micr}}(n^+)$ ) for the singly charged clusters; the method is described in detail elsewhere [22]. The corrections are added to the liquid drop predictions of **doubly** charged silver clusters. This procedure follows the assumption that the microscopic corrections depend only on the number of valence electrons, i.e.  $E_{\text{micr}}(n^{2+}) = E_{\text{micr}}((n-1)^+)$ . Thus, a semi-empirical macroscopic-microscopic model of doubly charged clusters can be established.

The resulting predictions for the dissociation energies of doubly charged silver clusters are shown in Fig. 4 (middle). The values for monomer evaporation reflect the measured dissociation energies of singly charged clusters, with the shell and odd-even effect shifted by one unit in cluster size. However, the calculated fission barriers show no odd-even-staggering: The microscopic corrections of initial and final states nearly cancel out (the initial cluster and the main fragment are both either odd or even- $n_e$  systems) and only shell effects remain. The measured dominant fragmentation pathways, e.g. the exceptional monomer evaporation of  $\text{Ag}_{11}^{2+}$  and  $\text{Ag}_{15}^{2+}$ , are correctly predicted by the macroscopic-microscopic model. Furthermore, a comparison between the measured dissociation energies of doubly charged clusters and the predicted ones shows a good quantitative agreement (Fig. 4 (bottom)). In particular the monotonic increase in the dissociation energies for the fissioning systems  $n = 12 - 16$  and the electronic shell at  $n = 10$  are well reproduced.

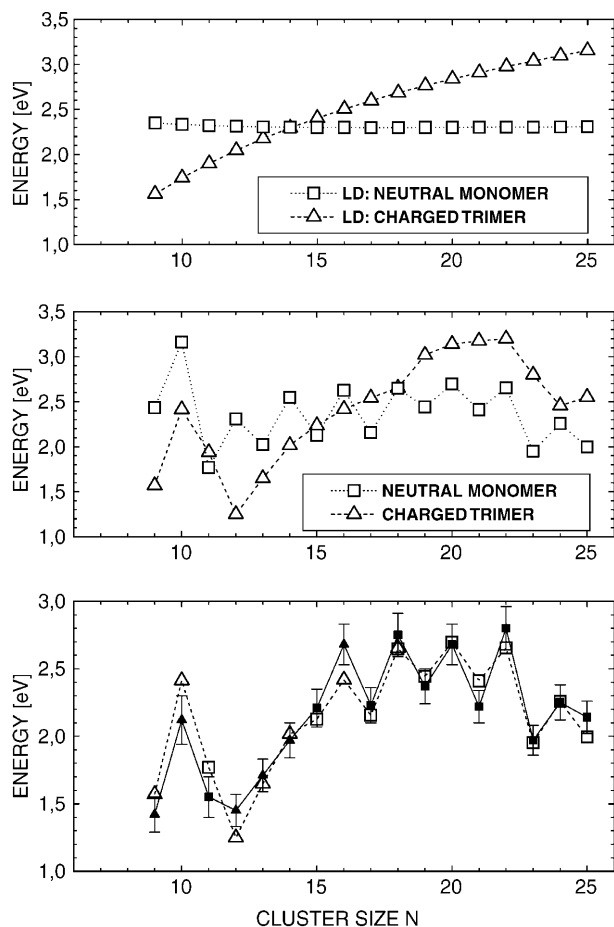


**Fig. 4.** Theoretical dissociation energies (open symbols) of doubly charged silver clusters (triangles for fission, squares for neutral monomer evaporation). (a) Top: Liquid drop model. (b) Middle: Liquid drop model with empirical microscopic corrections. (c) Bottom: Comparison between the dissociation energies as predicted from (b) and the experimental values (as in middle of Fig. 3, bold symbols).

## 5 Conclusion

In summary, the dissociation energies of doubly charged silver clusters have been measured and compared to those of singly charged silver clusters. Odd-even-staggering and shell effects have been found to depend only on the number of atomic valence electrons. Empirical microscopic corrections have been deduced from the measured dissociation energies of singly charged clusters and added to a macroscopic liquid-drop approach. Thus the measured dissociation energies and fission barriers of doubly charged clusters could be well reproduced.

Supported by the Deutsche Forschungsgemeinschaft (Schw 401/13), the Materialwissenschaftliches Forschungszentrum Mainz and the Fonds der Chemischen Industrie. S.K. acknowledges support by the Studienstiftung des deutschen Volkes.

## References

- O. Echt, T.D. Märk: in *Clusters of Atoms and Molecules II*, ed. by H. Haberland (Springer, Berlin, Heidelberg, New York 1994)
- U. Näher, S. Bjørnholm, S. Frauendorf, F. Garcias, C. Guet: *Phys. Rep.* **285**, 245 (1997)
- C. Bréchnignac, Ph. Cahuzac, F. Carlier, M. de Frutos: *Phys. Rev. Lett.* **64**, 2893 (1990); *Nucl. Instrum. Methods B* **88**, 91 (1994)
- W.A. Saunders: *Phys. Rev. Lett.* **64**, 3046 (1990); *Phys. Rev. A* **46**, 7028 (1992)
- L. Schweikhard, P. Beiersdorfer, W. Bell, G. Dietrich, S. Krückeberg, K. Lützenkirchen, B. Obst, J. Ziegler: *Hyperfine Interact.* **99**, 97 (1996)
- J. Ziegler, D. Dietrich, S. Krückeberg, K. Lützenkirchen, L. Schweikhard, C. Walther: *Hyperfine Interact.* **115**, 171 (1998)
- S. Krückeberg, G. Dietrich, K. Lützenkirchen, L. Schweikhard, C. Walther, J. Ziegler: *Hyperfine Interact.* **108**, 107 (1997); *Z. Phys. D* **40**, 341 (1997)
- I. Katakuse, H. Ito, T. Ichihara: *Int. J. Mass Spectrom. Ion Processes* **97**, 47 (1990); *Z. Phys. D* **20**, 101 (1991)
- C. Bréchnignac, P. Cahuzac, M. de Frutos, P. Garnier, N. Kebaïli: *Phys. Rev. B* **53**, 1091 (1996)
- J. Ziegler, G. Dietrich, S. Krückeberg, K. Lützenkirchen, L. Schweikhard, C. Walther: to be published
- S. Becker, K. Dasgupta, G. Dietrich, H.-J. Kluge, S. Kuznetsov, M. Lindinger, K. Lützenkirchen, L. Schweikhard, J. Ziegler: *Rev. Sci. Instrum.* **66**, 4902 (1995)
- L. Schweikhard, St. Becker, K. Dasgupta, G. Dietrich, H.-J. Kluge, D. Kreisle, S. Krückeberg, S. Kuznetsov, M. Lindinger, K. Lützenkirchen, B. Obst, C. Walther, H. Weidele, J. Ziegler: *Phys. Scr. T* **59**, 236 (1995)
- L. Schweikhard, S. Krückeberg, K. Lützenkirchen, C. Walther: *Eur. Phys. J. D*, this issue
- S. Krückeberg, P. Beiersdorfer, G. Dietrich, K. Lützenkirchen, L. Schweikhard, C. Walther: *Rapid Commun. Mass Spectrom.* **11**, 455 (1997)
- S. Krückeberg, G. Dietrich, K. Lützenkirchen, L. Schweikhard, C. Walther, J. Ziegler: *J. Chem. Phys.* **110**, 7216 (1999)
- E. Uggerud, P.J. Derrick: *J. Phys. Chem.* **95**, 1430 (1991)
- M.F. Jarrold, E.C. Honea: *J. Phys. Chem.* **95**, 9181 (1991)
- U. Hild, G. Dietrich, S. Krückeberg, M. Lindinger, K. Lützenkirchen, L. Schweikhard, C. Walther, J. Ziegler: *Phys. Rev. A* **57**, 2786 (1998)
- L.S. Kassel: *J. Phys. Chem* **32**, 225, 1065 (1928)
- S. Krückeberg, G. Dietrich, K. Lützenkirchen, L. Schweikhard, C. Walther, J. Ziegler: *Int. J. Mass Spectrom. Ion Processes* **155**, 141 (1996)
- M. Brack: *Rev. Mod. Phys.* **65**, 677 (1993); W.A. de Heer: *Rev. Mod. Phys.* **65**, 611 (1993)
- S. Krückeberg, G. Dietrich, K. Lützenkirchen, L. Schweikhard, C. Walther, J. Ziegler: *Phys. Rev. A*, in print
- M. Manninen, J. Mansikka-aho, H. Nishioka, Y. Takahashi: *Z. Phys. D* **31**, 259 (1994)
- V. Bonačić-Koutecký, L. Češpiva, P. Fantucci, J. Koutecký: *Z. Phys. D* **26**, 287 (1993)